applied sciences

MDPI

Article

Design and Performance Evaluation of a Flexible Lightweight Heating Blanket for Wind Turbine Blade Reinforcement

Jiaqi Lu [1], Xuan Cao [2], Guangjie Yang [2], Wanjuan Zhang [1], Yawen Wu [1], Hui Jiang [3] and Shaochun Tang [2,3,*]

[1] Sinoma Wind Power Blade (Jiuquan) Co., Ltd., Jiuquan 735000, China; lujq@sinomatech.com (J.L.); wwj5050@163.com (W.Z.); ruanquwei327@163.com (Y.W.)
[2] College of Engineering and Applied Sciences, Nanjing University, Nanjing 210023, China; 602023340026@smail.nju.edu.cn (X.C.); 602025340083@smail.nju.edu.cn (G.Y.)
[3] Haian Institute of High-Tech Research, Nanjing University, Haian 226600, China; ygj123@njfu.edu.cn
* Correspondence: tangsc@nju.edu.cn

Featured Application

A flexible carbon-nanotube-based heating blanket is developed for the in situ curing and reinforcement of wind turbine blade joint seams, offering rapid heating, high temperature uniformity, and conformal thermal management for large curved composite structures.

Abstract

The curing quality of epoxy resin at wind turbine blade joint seams critically affects blade integrity and service reliability, yet conventional metallic heating systems often suffer from poor temperature uniformity, limited flexibility, and slow thermal response. In this study, a flexible and lightweight heating blanket based on carbon nanotube (CNT) electrothermal film was developed for blade reinforcement and in situ curing applications. The device employs a multilayer composite architecture consisting of a CNT heating layer, a nano-aerogel thermal insulation layer, a thermoplastic polyurethane electrical insulation layer, and a silicone-coated glass fiber protective layer, together with an intelligent temperature control system. The resulting blanket, with a total thickness of 3.85 mm, exhibited rapid and stable heating performance, increasing from 25 to 120 °C within 8 min. Under resin-curing conditions, it achieved an initial heating rate of 7.2 °C min^{-1} and a temperature uniformity of ±2.6 °C, markedly outperforming a conventional Ni@Cr alloy heating blanket. Accelerated aging tests further demonstrated stable electrothermal performance under the tested condition. Those results indicate that the proposed CNT-based heating blanket provides an efficient and reliable thermal management strategy for large curved composite structures.

Keywords: wind turbine blades; carbon nanotube; epoxy resin curing; flexible heating blanket; thermal management

Check for updates

Academic Editor: Paolo Renna

Received: 13 April 2026
Revised: 29 May 2026
Accepted: 29 May 2026
Published: 30 June 2026

Copyright: © 2026 by the authors. Licensee MDPI, Basel, Switzerland. This article is an open access article distributed under the terms and conditions of the Creative Commons Attribution (CC BY) license.

1. Introduction

Against the backdrop of the global transition toward clean energy, wind power, as a mature and highly commercialized form of renewable energy, has experienced sustained and rapid growth in installed capacity [1,2]. As the primary components responsible for energy capture and conversion, wind turbine blades play a decisive role in the overall power generation efficiency, operational stability, and service life of wind turbines [3,4]. Those blades are typically manufactured using composite molding processes, in which the curing

of epoxy resin at the mold joint seams represents a critical step in the formation of high-strength structural interfaces [5]. The curing of epoxy resin involves a thermally activated physicochemical crosslinking process under prescribed temperature conditions, enabling the resin molecules to form a stable three-dimensional network structure. Adequate curing is therefore essential for minimizing the risks of seam cracking and structural failure during long-term blade operation [6,7].

Heating technologies for wind turbine blade curing were developed relatively early, with hot-air heating and infrared heating being among the initial methods employed [8]. At present, however, curing systems based on conventional metallic heating wires still suffer from several significant limitations. First, their heating uniformity is inadequate. Because heat is generated primarily at the wire surface, temperature distribution is often highly non-uniform, resulting in local overheating or insufficient curing. This can lead to incomplete resin crosslinking and defects such as residual voids, delamination, and interfacial weakness [9,10]. Second, metallic heating wires exhibit limited mechanical durability and adaptability. Prolonged service under elevated temperatures may accelerate oxidation and fatigue-induced fracture, thereby shortening their operational lifetime. Moreover, their inherent rigidity makes it difficult to achieve intimate contact with the complex curved surfaces of wind turbine blades, which can produce heating blind spots and exacerbate heat loss [11]. Third, their relatively high thermal inertia leads to slow heating and cooling responses, making precise temperature regulation during processing difficult to achieve. These shortcomings severely constrain both the manufacturing efficiency and quality stability of wind turbine blades [12]. To date, existing technologies have not fully addressed the core demands of precise temperature control, conformal heating over complex surfaces, and long-term reliability in blade reinforcement and curing applications [13,14].

To overcome those limitations, this study proposes an integrated thermal management solution through the design and development of a flexible heating blanket for wind turbine blade reinforcement based on carbon nanotube (CNT) electrothermal film. CNT film is considered an attractive candidate for next-generation heating elements because of its excellent electrical conductivity, thermal conductivity, flexibility, and chemical stability, as well as its advantages in rapid heating, uniform heat generation, controllability, and structural adaptability [15–17]. Owing to its planar heating mode, CNT film can provide more uniform heat distribution and conform closely to the curved geometry of blade joint seams, making it particularly suitable for complex processing scenarios [18–20]. In this work, a multilayer composite architecture integrating conductive, thermal-insulating, electrical-insulating, and protective functions was designed to achieve synergistic enhancement of the constituent materials. Specifically, the structure consists of CNT film as the heating layer, nano-aerogel felt as the thermal insulation layer, thermoplastic polyurethane (TPU) film as the electrical insulation layer, and silicone-coated glass fiber (GF) fabric as the outer protective layer. Through systematic experimental investigation, the heating characteristics, thermal equilibration behavior, and long-term service reliability of the developed heating blanket were comprehensively evaluated. This study provides an efficient, reliable, and energy-saving thermal management strategy for the curing of wind turbine blade mold joint seams, thereby supporting the advancement of blade manufacturing technology. The proposed approach is expected to offer significant engineering value for improving blade manufacturing and maintenance quality, reducing production costs, and promoting the intelligent and sustainable development of the wind power industry.

2. System Design and Material Selection

2.1. Overall Structural Design

The reinforcement heating blanket developed for wind turbine blades adopts a multilayer synergistic architecture, in which the functional layers are arranged sequentially from electrical conduction to thermal insulation, electrical isolation, and external protection. As summarized in Table 1, the blanket integrates multiple materials and functions within a compact composite structure. Specifically, it consists of a CNT film as the heating layer, supplemented with a silver-coated copper mesh for enhanced electrical conduction, a nano-aerogel felt as the thermal insulation layer, a TPU film as the electrical insulation layer, and a silicone-coated GF fabric as the outer protective layer. The total thickness of the entire structure is only 3.85 mm. This design not only ensures a lightweight configuration and excellent flexibility, but also enables intimate conformal contact with the complex curved surfaces of wind turbine blades.

Table 1. Materials, thicknesses, and functions of each layer in the wind turbine blade reinforcement heating blanket.

Hierarchy	Material	Thickness	Function
Conductive layer	CNT heating film with silver-coated copper mesh	0.25 mm	Reduce contact resistance and prevent local overheating
Insulation layer	Nano-aerogel felt (thermal conductivity ≤ 0.02 W m^{-1} K^{-1})	3.00 mm	Reduce heat loss and enhance energy efficiency
Insulation layer	TPU film	0.15 mm	Provide reliable electrical insulation
Outer Protective layer	Silicone-coated GF fabric	0.45 mm	Provide chemical resistance

As illustrated in Figure 1a, the CNT heating film is placed in close contact with the epoxy resin surface, thereby satisfying the requirement for uniform resin curing. The thermal insulation layer effectively suppresses heat dissipation while simultaneously reducing the influence of the external environment on the heating process. In addition, a quick-release connector is employed between the temperature controller and the heating element, allowing rapid detachment through a simple press-and-pull operation. This design facilitates convenient rolling, storage, and repeated reuse of the heating blanket. It should be noted that the dimensions of the reinforcement heating blanket can be tailored to specific application requirements.

Taking a 12 m $\times$ 0.8 m heating blanket for wind turbine blade reinforcement as a representative example, the circuit layout of the CNT heating film is presented in Figure 1b. A composite structural configuration was adopted, in which flexible TPU was used to encapsulate the CNT heating layer and ensure electrical insulation. The heating unit comprises multiple CNT film segments connected in parallel, a configuration that enhances temperature uniformity while mitigating the risk of local overheating. In addition, a composite electrode architecture integrating copper mesh and silver paste was introduced. The copper mesh serves as a conductive skeleton, offering both high electrical conductivity and mechanical support. Despite a thickness of only 0.05 mm, it provides sufficient structural integrity without compromising flexibility. The mesh surface was further coated with nanosilver paste to bridge intertube junctions within the CNT network and reduce interfacial contact resistance, thereby improving current transport and electrothermal performance.

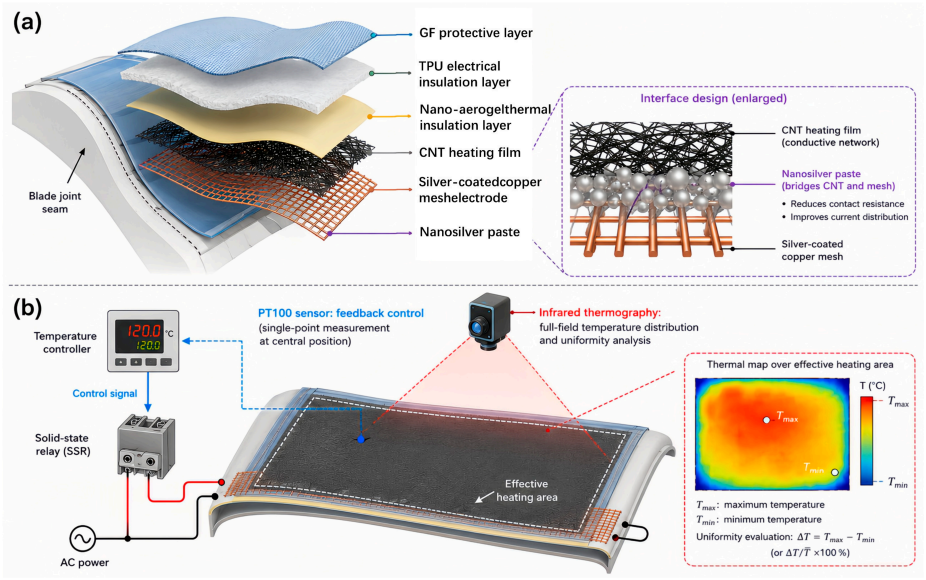

Figure 1. Schematic of the flexible CNT-based heating blanket for wind turbine blade reinforcement. (**a**) Multilayer structure and interfacial design. (**b**) Temperature sensing and thermal mapping strategy.

2.2. Layer-Specific Design

The heating functionality is enabled by a CNT electrothermal film fabricated using a chemical vapor deposition (CVD)-based process. As shown in Figure 2, the CNT electrothermal film exhibits a continuous and interconnected nanotube network. The surface SEM image reveals a randomly entangled CNT morphology, providing abundant conductive pathways for Joule heating [21,22]. The cross-sectional SEM image shows a layered CNT film with a thickness of approximately 12 μm, confirming the thin-film structure of the electrothermal layer. Owing to its tailored layered architecture, the film exhibits enhanced resistance to moisture ingress and chemical attack, contributing to improved service durability. More importantly, its intrinsic flexibility allows intimate conformal contact with curved blade surfaces, thereby promoting spatially uniform and efficient heat transfer across complex geometries. To further optimize electrothermal behavior, a composite electrode consisting of silver-coated copper mesh and nanosilver paste was employed. The copper mesh provides a robust conductive framework, whereas the nanosilver paste fills interstitial regions between adjacent CNTs, thereby lowering contact resistance and improving both current distribution and heating homogeneity. The incorporation of silver also benefits heat transfer because of its high electrical and thermal conductivity.

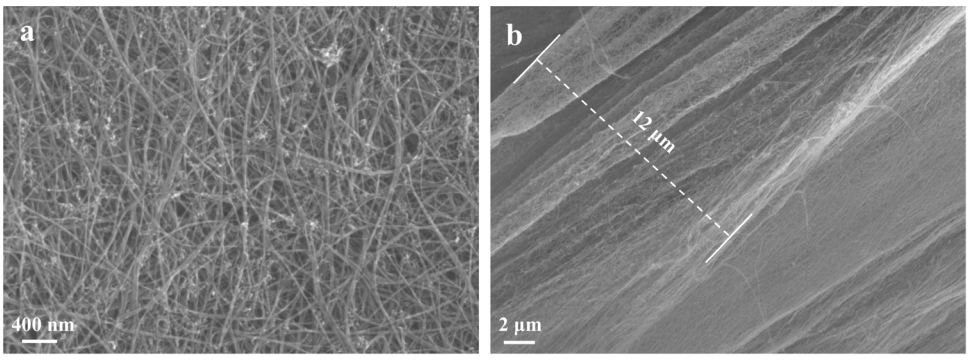

Figure 2. SEM images of the CNT electrothermal film. (**a**) Surface morphology showing the interconnected CNT network. (**b**) Cross-sectional image of the CNT film.

Thermal insulation was achieved using a 3 mm thick nano-aerogel felt with a thermal conductivity not exceeding 0.02 W m^{-1} K^{-1} [23]. This material effectively suppresses parasitic heat dissipation from the heating blanket to non-target regions, thereby enhancing thermal utilization efficiency and reducing energy loss during curing. Electrical insulation and encapsulation were provided by a 0.15 mm thick TPU film. With a dielectric strength of no less than 20 kV mm^{-1}, the TPU layer ensures reliable electrical isolation of the heating element. Meanwhile, its favorable flexibility and thermal resistance make it particularly suitable for deformable heating systems designed to accommodate complex curved surfaces.

The outermost protective layer consists of a 0.45 mm thick silicone-coated GF fabric. This material combines low weight, mechanical robustness, flexibility, and thermal resistance, thereby providing effective protection for the internal functional layers. In addition, it facilitates demolding after epoxy curing, which enhances the practical operability and reusability of the heating blanket in engineering applications.

2.3. Temperature Control System

The temperature control system architecture of the wind turbine blade reinforcement heating blanket is shown in Figure 3. The system consists of a PT100 thin-film temperature sensor, a temperature controller, a 25 A solid-state relay, and the CNT-based heating blanket. The PT100 sensor was attached to the working surface of the heating blanket to monitor the surface temperature and provide feedback to the controller. The temperature controller regulated the power supply to the heating blanket through the solid-state relay, enabling closed-loop temperature control during the heating and curing process. The PT100 thin-film sensor has a response time of approximately 3 s, allowing rapid detection of temperature fluctuations. The 25 A solid-state relay was selected to match the power demand of the representative full-size heating blanket. For the 4 kW system, the operating current was approximately 9.5 A, which remained within the rated capacity of the relay and provided a sufficient safety margin.

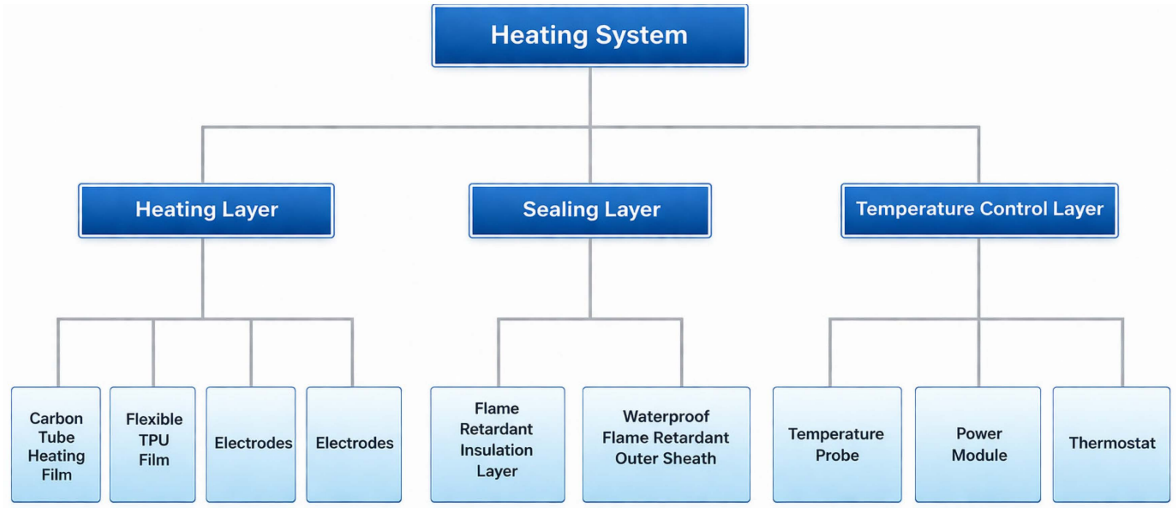

Figure 3. Temperature control system architecture of wind turbine blade reinforcement heating blanket.

2.4. Preparation Process Flow

The fabrication of the heating blanket involved four sequential steps. First, the CNT film continuously produced by the CVD process was integrated with a silver-coated copper mesh electrode using nanosilver slurry, thereby establishing a complete conductive heating circuit. Second, the resulting composite heating layer was encapsulated between two TPU films through hot pressing to form an electrically insulated and moisture-resistant heating

core. Third, the heating core, nano-aerogel thermal insulation layer, and silicone-coated glass fiber fabric outer protective layer were assembled into a multilayer structure, followed by lamination and hot-press curing using a high-temperature-resistant adhesive to obtain the final integrated flexible heating blanket. Finally, a PT100 temperature sensor and waterproof connector were installed, and the assembled system was commissioned in conjunction with the temperature controller.

3. Experimental Scheme and Performance Test

3.1. Temperature Rise and Thermal Balance Performance Test

At an ambient temperature of 25.5 °C, an input voltage of 220 V was applied to three heating blankets with different structural configurations, and their thermal responses were monitored for 20 min. The reported heating rate, equilibrium temperature, and thermal equilibrium time were obtained as average values from repeated temperature measurements under the same test conditions. Heating blanket A consisted of silicone-coated glass fiber fabric (Nanjing Fiberglass Research & Design Institute, Nanjing, China), nano-aerogel felt (XFNANO Materials Tech Co., Ltd., Nanjing, China), and CNT film (XFNANO Materials Tech Co., Ltd., Nanjing, China), corresponding to the design proposed in this study. Heating blanket B consisted of silicone-coated glass fiber fabric and CNT film without a thermal insulation layer. Heating blanket C was a conventional Ni@Cr alloy heating blanket (Danyang Haiwei Electric Heating Alloy Co., Ltd., Danyang, China) used as the reference sample.

As shown in Figure 4, heating blanket A exhibited the fastest temperature rise among the three configurations. It required only 8 min to increase from 25 to 120 °C, whereas heating blanket C required 13 min to reach the same temperature. Accordingly, the average heating rate of heating blanket A over this interval was approximately 11.9 °C min^{-1}, markedly higher than that of heating blanket C (approximately 7.3 °C min^{-1}). In addition to its faster transient response, heating blanket A also reached a higher steady-state temperature, approaching thermal equilibrium at approximately 125 °C. By contrast, heating blanket C attained a similar equilibrium temperature of 124 °C only after a substantially longer heating period. These results indicate that the CNT-based heating blanket enables faster heating than the conventional Ni@Cr system while maintaining comparable thermal stability near the target curing temperature. Heating blanket B exhibited a distinctly different thermal response. Although its temperature increased continuously during the initial stage of heating, it failed to reach 120 °C within the test period and instead stabilized at approximately 102 °C. This behavior highlights the critical role of the nano-aerogel felt in suppressing heat loss and improving thermal utilization efficiency. In the absence of the thermal insulation layer, a considerable fraction of the input energy was dissipated to the surroundings, preventing the blanket from meeting the temperature requirement for resin curing.

The superior performance of heating blanket A can be attributed to the synergistic integration of the CNT planar heating layer and the nano-aerogel thermal insulation layer. The three-dimensional conductive network formed by the CNTs provides high electrothermal conversion efficiency and low thermal mass, enabling rapid heat generation under electrical excitation. Meanwhile, the planar heating mode of the CNT film is inherently more favorable for spatially uniform heat delivery than conventional wire-based heating. The lightweight multilayer architecture further reduces the overall thermal inertia of the system, while the nano-aerogel felt minimizes parasitic heat dissipation and promotes heat retention at the working surface.

As further summarized in Table 2, heating blanket A outperformed the two reference structures in terms of heating rate, attainable temperature, and effective thermal reten-

tion. These results demonstrate that the performance enhancement cannot be attributed to a mere additive combination of constituent materials, but rather to the functional synergy between the CNT electrothermal film and the nano-aerogel insulation layer. Specifically, the CNT film provides rapid and efficient planar heat generation, whereas the nano-aerogel felt suppresses outward heat loss and concentrates thermal energy within the target curing region. Their combination enables rapid heating, effective heat retention, and improved thermal response, making the proposed structure particularly suitable for epoxy curing in wind turbine blade joint reinforcement. For the representative 12 m × 0.8 m heating blanket with an input power of 4 kW, the effective heating area is 9.6 m^2, corresponding to an areal power density of approximately 416.7 W m^{-2}. This value was sufficient to reach the target temperature under the laboratory conditions used in this study. In low-ambient-temperature wind farm environments, higher power density or improved thermal insulation may be required to compensate for increased heat loss. Compared with conventional nichrome-wire heating blankets, the CNT-based planar heating structure provides faster thermal response and improved surface temperature uniformity. The integrated nano-aerogel insulation layer further helps reduce heat dissipation, supporting its applicability to large curved composite structures.

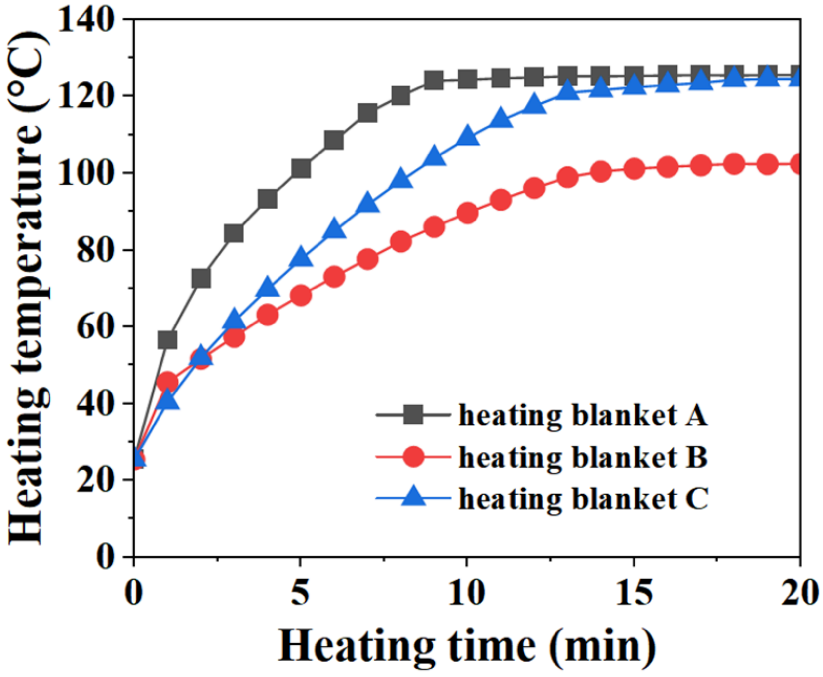

Figure 4. Temperature-rise curves of heating blankets with different structural configurations.

Table 2. Heat balance performance results.

Performance Parameters	Heating Blanket A	Heating Blanket B	Heating Blanket C
Rise time from 25 to 120 °C in bare-blanket test (min)	8	/	13
Heating-area equilibrium temperature (°C)	125	102	124
Thermal equilibrium time (min)	9	16	18

For comparison with reported flexible electrothermal systems, the present heating blanket provides large-area heating over 9.6 m^2 with an areal power density of approximately 416.7 W m^{-2}. Previous CNT-film-based composite-curing systems and carbon-based flexible de-icing heaters have demonstrated the feasibility of resistive Joule heating for

composite processing and low-temperature surface heating [14,17,18,21,22]. Compared with these systems, the present design emphasizes large-area conformal heating for curved wind turbine blade structures, while the integrated nano-aerogel insulation layer helps reduce heat loss and maintain the target curing temperature.

3.2. Resin Curing Performance Test

In the resin-curing test, a commercial epoxy resin system for wind turbine blade joint reinforcement was adopted. The epoxy resin and hardener were mixed at a mass ratio of 100:30 according to the manufacturer-recommended formulation. The mixture was then applied onto the glass-fiber-reinforced composite substrate. To further evaluate the heating performance of the proposed blanket under practical resin-curing conditions, an epoxy resin curing experiment was conducted. The curing duration was set to 120 min. Heating blanket A, based on the CNT electrothermal film, and heating blanket C, based on conventional Ni@Cr alloy heating blanket, were selected for comparison. The temperature evolution of the two heating blankets during the curing process was continuously monitored. In addition, temperature data at four representative time points, namely 30, 60, 90, and 120 min, were extracted for comparative analysis. During the initial stage of resin curing, heating blanket A exhibited a markedly faster thermal response than heating blanket C. As listed in Table 3, the heating rate of heating blanket A during the first 5 min reached 7.2 °C min^{-1}, whereas that of heating blanket C was only 2.6 °C min^{-1}, approximately 64% lower. This substantial difference indicates the superior electrothermal conversion capability of the CNT heating film, which enables thermal energy to be rapidly delivered to the working region and effectively shortens the preheating stage of the curing process. A more pronounced advantage of heating blanket A was observed in terms of temperature uniformity.

Table 3. Indicators of Heating Pad Curing Performance.

Performance Indicators	Heating Blanket A	Heating Blanket C
Heating rate (0–5 min)/°C min^{-1}	7.2	2.6
Temperature uniformity/°C	±2.6	±8.3
Steady-state temperature at 40 min/°C	75	72

As shown in Figure 5, the CNT heating blanket exhibited a markedly faster thermal response than the conventional Ni@Cr alloy heating blanket during epoxy resin curing. The temperature of the CNT-based system increased rapidly during the initial heating stage and approached a stable plateau after approximately 20–25 min, whereas the Ni@Cr alloy heating blanket required a substantially longer period to reach a comparable temperature level. This result indicates that the CNT heating blanket can establish the curing temperature field more rapidly, thereby shortening the preheating stage of the curing process. Notably, both systems eventually reached a similar steady-state temperature of approximately 73–75 °C, suggesting that the main advantage of the CNT-based design lies not in a higher final temperature, but in its faster heating kinetics and earlier stabilization. This superior transient performance can be attributed to the high electrothermal conversion efficiency, low thermal inertia, and planar heating mode of the CNT film, which enable faster and more effective heat delivery to the curing region than the conventional wire-based heating mechanism.

These results demonstrate that the CNT-based heating blanket provides substantially more homogeneous heat distribution during resin curing. Such improved temperature uniformity is critical for preventing local over-curing or insufficient curing of the epoxy resin, both of which may compromise bonding quality and structural integrity. In addition, heating blanket A exhibited a steady-state temperature of 75 °C at 40 min, slightly higher

than the 72 °C measured for heating blanket C, indicating better compliance with the thermal requirements of the curing process. Taken together, these results confirm that, compared with the conventional wire-based system, the CNT heating blanket offers clear advantages in heating rate, temperature uniformity, and process stability, making it more suitable for wind turbine blade reinforcement applications.

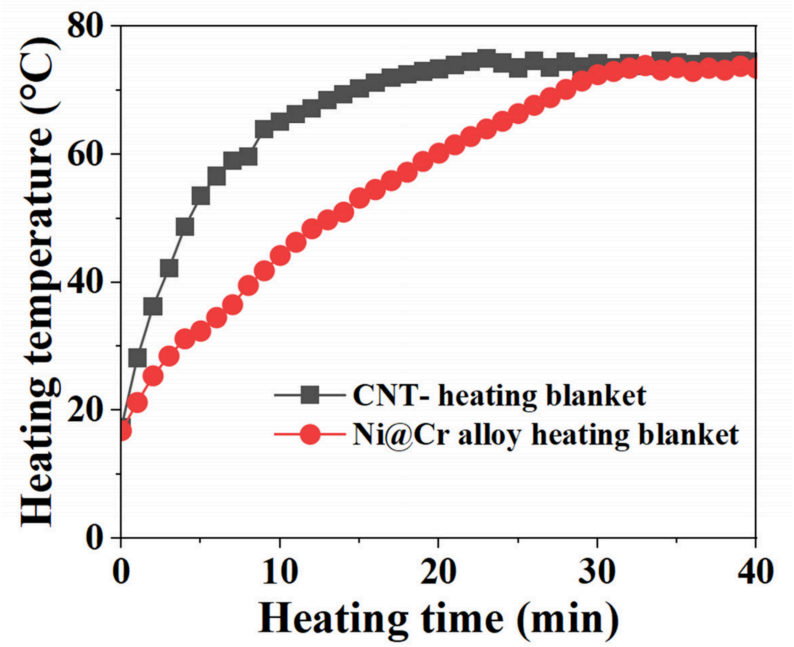

Figure 5. Temperature-rise curves of the CNT-based heating blanket and the conventional nichrome-wire heating blanket during the resin-curing test.

Infrared thermography was used to evaluate the spatial temperature distribution of the heating blankets during the resin-curing test. Thermal images were analyzed at 30, 60, 90, and 120 min. For each image, the maximum temperature T_{max} and minimum temperature T_{min} within the selected effective heating area were extracted, and the spatial temperature difference was calculated as $\Delta T = T_{max} - T_{min}$. The temperature uniformity was expressed as $\pm$[mean(ΔT)]/2. Based on the four selected time points, the average ΔT values of heating blanket A and heating blanket C were 5.23 °C and 16.63 °C, respectively, corresponding to average temperature uniformities of $\pm$2.6 °C and $\pm$8.3 °C. As shown in Figure 6, after 30 min of curing, the temperature difference across heating blanket C reached 19.6 °C, whereas that of heating blanket A was only 2.5 °C. At 60 min, the corresponding temperature differences were 14.3 and 8.5 °C, respectively. After 90 min, the temperature difference in heating blanket C increased to 17.0 °C, while heating blanket A maintained a much smaller value of 4.4 °C. Even at 120 min, the temperature difference in heating blanket C remained as high as 15.6 °C, compared with only 5.5 °C for heating blanket A. Overall, the temperature uniformity of heating blanket A was calculated to be $\pm$2.6 °C, which is markedly better than the $\pm$8.3 °C obtained for heating blanket C. These results demonstrate that heating blanket A provides substantially more uniform heat distribution during the resin-curing process. Such improved thermal uniformity is essential for avoiding local over-curing or insufficient curing of the epoxy resin, both of which may compromise curing consistency and structural performance. In addition, heating blanket A exhibited a more appropriate steady-state temperature and a smaller fluctuation range, indicating better compliance with the thermal requirements of epoxy curing. Collectively, these results confirm that the CNT-based heating blanket is more capable of ensuring uniform and stable curing than the Ni@Cr alloy heating blanket. It should be noted that

the infrared thermography analysis mainly reflects the surface temperature distribution of the heating blanket. During epoxy curing, a through-thickness thermal lag may exist between the blanket surface and the internal resin/composite joint, especially during the initial heating stage.

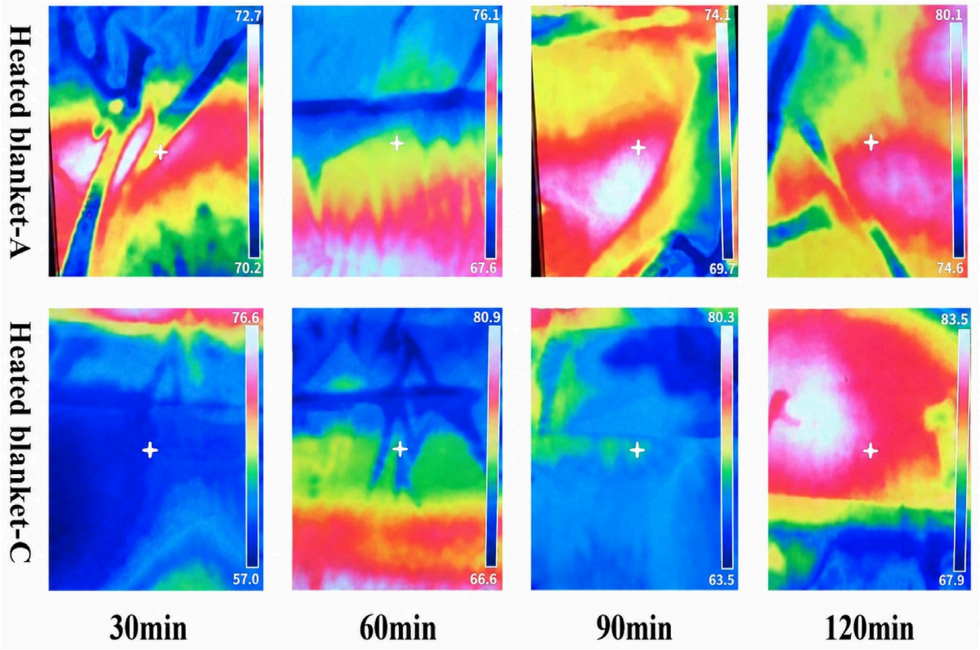

Figure 6. Infrared thermal images of heating blanket A and heating blanket C during the resin-curing test at 30, 60, 90, and 120 min. The color scale represents the surface temperature distribution, with warmer colors indicating higher temperatures and cooler colors indicating lower temperatures. The white cross/diamond mark indicates the reference point displayed by the infrared camera.

Practical application tests were further conducted to assess the feasibility of the proposed heating blanket in real blade reinforcement scenarios. The blanket exhibited good portability and ease of deployment owing to its lightweight and flexible structure (Figure 7a). When applied to the wind turbine blade surface, it closely conformed to the curved joint region without obvious detachment or geometric mismatch, indicating excellent surface compatibility and installation adaptability (Figure 7b). Those results provide direct evidence for the practical utility of the developed system in the in situ curing and reinforcement of large-scale wind turbine blades.

3.3. Interfacial Peeling Resistance and Mechanical Durability

The accelerated aging performance of the CNT heating element was evaluated by a third-party test conducted by the Wuhan Product Quality Supervision and Inspection Institute. A coupon-scale CNT heating film sample was continuously operated at 297 V for 36 h. As summarized in Table 4, the input power changed from 104.53 W to 105.21 W after aging, corresponding to a variation of approximately 0.65%. No visible damage, leakage-current increase, or dielectric breakdown was observed. The sample also met the acceptance criteria listed in Table 4, including leakage current $\leq$ 3.5 mA and no dielectric breakdown under 1500 V for 1 min, with reference to IEC 60335-2-17 [24]. It should be noted that this accelerated aging test was performed on a coupon-scale CNT heating film sample rather than the full-size 4 kW heating blanket. Therefore, the aging result mainly reflects the electrothermal stability of the CNT heating film under the tested accelerated condition. For the full-size heating blanket, additional factors such as large-area current

distribution, edge effects, electrode contact resistance, and non-uniform heat dissipation may further influence long-term electrical and thermal stability.



Figure 7. Practical application of the flexible CNT-based heating blanket. (**a**) Before deployment; (**b**) after deployment on the blade surface.

Table 4. Key data of accelerated aging test of carbon nanotube heating film.

Test Parameter	Before Aging	After Aging	Acceptance Criterion	Assessment
Input power (W)	104.53	105.21	/	Pass
Appearance	No visible damage or deformation	No visible melting, rupture or deformation	No damage	Pass
Power deviation (%)	0.1	0.2	±15	Pass
Leakage current (mA)	<0.02	<0.02	≤3.5	Pass
Electrical strength	No breakdown	No breakdown	No breakdown under 1500 V for 1 min	Pass

The durability of the outer protective layer was assessed by interfacial peel testing. The initial peel force of the silicone outer layer was 7.5 N cm^{-1}, and it changed slightly to 7.9 N cm^{-1} after 50 simulated assembly–disassembly cycles. The peel force remained below the failure threshold of 15 N cm^{-1}, indicating that the silicone-coated glass fiber protective layer maintained stable interfacial adhesion under the tested repeated handling condition. These results provide a preliminary indication of the reusability and mechanical robustness of the outer protective layer [25,26]. The electrical resistance stability of the CNT conductive network under repeated mechanical flexing should also be considered for conformal deployment on curved blade surfaces. Cyclic bending may affect CNT–CNT contact and CNT/electrode interfacial contact, potentially causing resistance fluctuation or local current concentration. The interconnected CNT network, silver-coated copper mesh, nanosilver paste interface, and TPU encapsulation are expected to help maintain electrical continuity and reduce local resistance variation during conformal deployment.

4. Conclusions

A flexible CNT-film-based heating blanket for wind turbine blade reinforcement was developed in this study. By integrating planar CNT electrothermal heating with

nano-aerogel thermal insulation in a multilayer composite architecture, the proposed system effectively overcomes the major limitations of conventional wire-based heating, particularly poor temperature uniformity, high heat loss, and limited durability. The developed heating blanket exhibited rapid thermal response and stable curing performance, reaching 120 °C from 25 °C within 8 min. During epoxy curing, it achieved a heating rate of 7.2 °C min^{-1} in the initial 5 min and maintained a temperature uniformity of ±2.6 °C, markedly outperforming the Ni@Cr alloy heating blanket. In addition, accelerated aging and peel-resistance tests confirmed its good durability and engineering applicability. Overall, the proposed heating blanket provides an efficient, lightweight, and reliable thermal management solution for wind turbine blade seam curing. The present work demonstrates the potential of CNT-based flexible electrothermal systems for improving blade manufacturing quality and process efficiency, and offers a promising strategy for broader applications in large-scale composite curing.

Author Contributions: Conceptualization, J.L. and S.T.; methodology, J.L., X.C. and G.Y.; software, X.C.; validation, J.L., W.Z., Y.W. and H.J.; formal analysis, X.C. and G.Y.; investigation, J.L., W.Z., Y.W. and H.J.; resources, W.Z., Y.W. and S.T.; data curation, X.C. and G.Y.; writing—original draft preparation, J.L. and X.C.; writing—review and editing, G.Y., H.J. and S.T.; visualization, X.C. and G.Y.; supervision, S.T.; project administration, S.T. and J.L.; funding acquisition, S.T. All authors have read and agreed to the published version of the manuscript.

Funding: This work was supported by the National Key Research and Development Program of China (No. 2022YFA1602700), the National Natural Science Foundation of China (22375089), and the Gansu Provincial Science and Technology Program (No. 25YFGF001).

Institutional Review Board Statement: Not applicable.

Informed Consent Statement: Not applicable.

Data Availability Statement: The data can be obtained from the corresponding author according to reasonable requirements. The data are not publicly available due to privacy concerns.

Conflicts of Interest: Authors Jiaqi Lu, Wanjian Zhang, and Yawen Wu were employed by the company Sinoma Wind Power Blade (Jiuquan) Co., Ltd. The remaining authors declare that the research was conducted in the absence of any commercial or financial relationships that could be construed as a potential conflict of interest.

References

1. Jin, H.; Li, Y.; Wang, B.; Yang, B.; Jin, H.; Cao, Y. Adaptive forecasting of wind power based on selective ensemble of offline global and online local learning. *Energy Convers. Manag.* **2022**, *271*, 116296. [CrossRef]
2. Liu, P.; Li, M.; Han, C.; Meng, L.; Shao, Z. From input to output: Unraveling the Spatio-temporal pattern and driving factors of the coupling coordination between wind power efficiency and installed capacity in China. *Appl. Energy* **2025**, *396*, 126320.
3. Johnson, S.B.; Chetan, M.; Griffith, D.T.; Sherwood, J. A design-driven wind blade manufacturing model to identify opportunities to reduce wind blade costs. *Renew. Energy* **2023**, *215*, 118945. [CrossRef]
4. Bahru, T.B.; Kule, T.D.; Getachew, N.A.; Berry, H.D.; Wang, C.; Hu, P.; Liu, Y. Chemical recycling wind turbine blades for green future. *Renew. Sustain. Energy Rev.* **2026**, *232*, 116845. [CrossRef]
5. Sam-Daliri, O.; Jiang, Y.; Flaherty, D.; Walls, M.; Kennedy, C.; Flanagan, M.; Ghabezi, P.; Finnegan, W. Mechanical analysis of unidirectional glass fibre reinforced epoxy composite joints manufactured by adhesive bonding and co-curing techniques. *Mater. Des.* **2025**, *258*, 114739. [CrossRef]
6. Zhang, J.; Zhang, Z.; Huang, R.; Tan, L. Advances in Toughening Modification Methods for Epoxy Resins: A Comprehensive Review. *Polymers* **2025**, *17*, 1288. [CrossRef] [PubMed]
7. Schaible, P.; Schwaiberger, D.; Schabel, S.; Fleischer, J. Cure Modelling and Monitoring for Isothermal Processing of Fast-Curing Epoxy Resin. *Polymers* **2026**, *18*, 952. [CrossRef] [PubMed]
8. Abdi, B.; Tehrani-Bagha, A.R. Toward Robust Electrical Heating Textiles: Factors Influencing Electrical Heating Performance and Durability. *ACS Omega* **2025**, *10*, 51354–51367. [CrossRef] [PubMed]

9. Jing, Z.; Hong, M. Electromagnetic induction heating assisted laser cleaning of metal oxide layer. *Appl. Phys. A* **2024**, *131*, 24–31. [CrossRef]
10. Luo, J.; Lu, H.; Zhang, Q.; Yao, Y.; Chen, M.; Li, Q. Flexible carbon nanotube/polyurethane electrothermal films. *Carbon* **2016**, *110*, 343–349. [CrossRef]
11. Kang, K.-J. A wire-woven cellular metal of ultrahigh strength. *Acta Mater.* **2009**, *57*, 1865–1874. [CrossRef]
12. Mishnaevsky, L., Jr.; Frost-Jensen Johansen, N.; Fraisse, A.; Fæster, S.; Jensen, T.; Bendixen, B. Technologies of Wind Turbine Blade Repair: Practical Comparison. *Energies* **2022**, *15*, 1767. [CrossRef]
13. Bointon, T.H.; Barnes, M.D.; Russo, S.; Craciun, M.F. High Quality Monolayer Graphene Synthesized by Resistive Heating Cold Wall Chemical Vapor Deposition. *Adv. Mater.* **2015**, *27*, 4200–4206. [CrossRef] [PubMed]
14. Xu, X.; Zhang, Y.; Jiang, J.; Wang, H.; Zhao, X.; Li, Q.; Lu, W. In-situ curing of glass fiber reinforced polymer composites via resistive heating of carbon nanotube films. *Compos. Sci. Technol.* **2017**, *149*, 20–27. [CrossRef]
15. Cha, J.; Jin, S.; Shim, J.H.; Park, C.S.; Ryu, H.J.; Hong, S.H. Functionalization of carbon nanotubes for fabrication of CNT/epoxy nanocomposites. *Mater. Des.* **2016**, *95*, 1–8. [CrossRef]
16. Feng, J.; Wang, P.; Bai, Y.; Chen, X.; Li, T.; Luo, X.; Zhang, P.; Wang, X. Design of Highly Conductive Leather Based on Zirconium Ion Coordination for Health Protection in Severe Harsh Conditions. *Adv. Mater. Technol.* **2023**, *8*, 2301304. [CrossRef]
17. Kostaras, C.; Pavlou, C.; Koutroumanis, N.; Paterakis, G.; Trakakis, G.; Galiotis, C.; Dassios, K. Rapid Resistive Heating in Graphene/Carbon Nanotube Hybrid Films for De-icing Applications. *ACS Appl. Nano Mater.* **2023**, *6*, 5155–5167.
18. Zheng, B.; Wang, H.; Wu, X.; Yang, K.; Yu, Y.; Cui, H.; Gao, F.; Qian, K.; Yao, H.; Li, J.; et al. Flexible nanocomposite electrothermal films based on carbon nanotubes and waterborne polyurethane with high reliability, stretchability and low-temperature performance for wind turbine blade deicing. *Compos. Part A Appl. Sci. Manuf.* **2022**, *158*, 106979. [CrossRef]
19. Pang, J.; Qiu, W.; Meng, Q.; Zhou, J.; Wang, X.; Yue, Y. Design and Research of an Aircraft Ice Control System Based on Multilayer Functional Film. *Adv. Eng. Mater.* **2025**, *27*, 2402352. [CrossRef]
20. Zhang, Y.; Huang, X.; Zhou, J.; Liang, W.; Li, X.; Zhu, C. Durable Metallized Liquid Crystal Polymer Fibers Enable Flexible and Tough Electrical Heaters. *Polymers* **2025**, *17*, 1087. [CrossRef] [PubMed]
21. Huang, Z.; Li, S.; Guo, H.; Huang, C.; Bian, Y.; Gong, Y.; Huang, J.; Zeng, Q. Multi-scale GO/CNT/AlN nanocomposites for high-performance flexible electrothermal film heaters. *J. Mater. Chem. C* **2023**, *11*, 9925–9936.
22. Jia, S.L.; Geng, H.Z.; Wang, L.; Tian, Y.; Xu, C.X.; Shi, P.P.; Gu, Z.Z.; Yuan, X.S.; Jing, L.C.; Guo, Z.Y.; et al. Carbon nanotube-based flexible electrothermal film heaters with a high heating rate. *R. Soc. Open Sci.* **2018**, *5*, 172072. [CrossRef] [PubMed]
23. Hoseini, A.; Malekian, A.; Bahrami, M. Deformation and thermal resistance study of aerogel blanket insulation material under uniaxial compression. *Energy Build.* **2016**, *130*, 228–237. [CrossRef]
24. *IEC 60335-2-17:2022*; Household and Similar Electrical Appliances—Safety—Part 2-17: Particular Requirements for Blankets, Pads, Clothing and Similar Flexible Heating Appliances. International Electrotechnical Commission: Geneva, Switzerland, 2022.
25. *ASTM D903-98:2017*; Standard Test Method for Peel or Stripping Strength of Adhesive Bonds. ASTM International: West Conshohocken, PA, USA, 2017.
26. *ISO 8510-2:2006*; Adhesives—Peel Test for a Flexible-Bonded-to-Rigid Test Specimen Assembly—Part 2: 180 Degree Peel. International Organization for Standardization: Geneva, Switzerland, 2006.

Disclaimer/Publisher's Note: The statements, opinions and data contained in all publications are solely those of the individual author(s) and contributor(s) and not of MDPI and/or the editor(s). MDPI and/or the editor(s) disclaim responsibility for any injury to people or property resulting from any ideas, methods, instructions or products referred to in the content.